

On the shape of active region coronal loops observed by Hinode/EIS.

P. Syntelis¹, C. Gontikakis¹, C.E. Alissandrakis², M. Georgoulis¹, K. Tsinganos^{3,4}

¹Research Center for Astronomy and Applied Mathematics, Academy of Athens

²Section of Astro-Geophysics, Department of Physics, University of Ioannina

³National Observatory of Athens

⁴Section of Astrophysics, Astronomy and Mechanics Department of Physics, University of Athens

Abstract: We study plasma flows in NOAA Active Region (AR) 10926, observed on December 3, 2006 with Hinode's EUV Imaging Spectrograph (EIS). We measured the line-of-sight velocity of coronal loops in the Fe VIII 185Å, Fe X 184Å, Fe XII 195Å, Fe XIII 202Å, and Fe XV 284Å spectral lines and reconstructed the three dimensional (3D) shape and velocity of plasma flow using a simple geometrical model. A magnetic field extrapolation was also carried out in order to identify magnetic field lines corresponding to the reconstructed 3D loops.

1 Introduction

Solar telescopes provide us with two-dimensional projections of coronal structures on the plane of the sky. Here we use the method developed by Alissandrakis et al (2008) to reconstruct the 3D loop profile. We applied this method to a number of loops using data from the Hinode/EIS spectrograph. Furthermore, we used magnetic field extrapolations, derived from photospheric magnetograms, to compare our results with the computed magnetic field geometry.

For this study, we treated NOAA Active Region (AR) 10926 EIS data, recorded in Fe VIII 185Å, Fe X 184Å, Fe XII 195Å, Fe XIII 202Å, and Fe XV 284Å spectral lines (Del Zanna, 2008), during two different rasters. Raster 1 was obtained from 15:32:19 UT to 17:46:31 UT with a 256'' × 256'' field of view (f.o.v.), while raster 2 was obtained from 19:15:12 UT to 23:44:09 UT and covered a 512'' × 256'' f.o.v. Both rasters were scanned from East to West with a 30s exposure time with a 1'' spatial resolution.

Magnetic field extrapolations were computed (Alissandrakis, 1981) using SOT/Spectropolarimeter and SOHO/MDI magnetograms. We performed force-free magnetic field extrapolations with constant α in order to find values of α for which the extrapolated field lines best fit the observed loops.

2 Reconstruction Model

From the aforementioned EIS data we selected for each wavelength the loops that could be distinguished from the background along their entire length (Figure 1 panel a). Measurements of the loops' position and line-of-sight velocity were then used as input for the computation of the 3D structure of the selected loops (Figure 1 panels b,c; see also Alissandrakis et al 2008). Assuming that the loop lies on a plane, we used a number of plane inclinations β with respect to the vertical plane on the solar surface (bounded between two extreme values β_1 and β_2 , so that the loop is not submerged). Then we transformed the loop coordinates and the line of sight velocities from the plane-of-sky coordinate system to the loop-plane reference system assuming that the velocity vector is always tangent to the loop. The optimal value of β is then chosen using as a criterion the continuity of the flow along the loop (Figure 1 panels d,e).

3 Conclusions

A) Loop 3D reconstruction was performed for 12 loops at raster 1 and 13 loops at raster 2. From those, only 9 loops from the former and 8 loops from the latter raster gave acceptable results, in the

Table 1: Summary of results for the loop shown in Figure 1, for all wavelengths and both time frames. Columns 1,2) Spectral line and formation temperatures. Columns 3,4) Inclination (β) and type of plasma motion observed in each spectral line during raster 1 and 2.

lines	logT (K)	Raster 1 β and motion	Raster 2 β and motion
Fe VIII 185Å	5.8	60° East to West	63° East to West
Fe X 184Å	6.0	64° Draining motion	61° Draining Motion
Fe XII 195Å	6.1	64° Draining motion	61° West to East
Fe XIII 202Å	6.2	65° West to East	54° West to East
Fe XV 284Å	6.3	–	62° West to East

sense that there were values of β for which velocity was found to be continuous. These loops were observed to have draining flows or unidirectional flows, and inclinations which were large in general (59° to 72°).

C) Time difference of 4 hours between the two rasters does not appear to affect the flows. Five loops were observed in both time frames. In four of them the direction of the flow did not change: the draining motion continued, and the unidirectional flows were sustained. In the case presented here (Fig. 1), the draining flow (in raster 1) appears to have transformed to unidirectional (in raster 2).

D) At each wavelength and for both time frames, there seems to exist a preference for a particular kind of flow. At Fe X 184Å, 3 out of 4 loops have a draining flow. At Fe VIII 185Å, all 3 observed loops have flows from East to West. At Fe XII 195Å, 3 out of 4 loops have a draining motion. At Fe XIII 202Å, all 4 observed loops have flows from the West footpoint to the East. At Fe XV 284Å, for which we were able to get results only at raster 2, both observed loops have flows from the West to the East footpoint.

E) The same loop, when seen in different spectral lines at the same time, can have different flows and in some cases different inclinations.

F) The comparison of the magnetic lines with the loops had moderate success. The best results were obtained for left-handed (negative) alphas in all cases. This was done using the magnetic flux weighted method of finding the most suitable alpha for an area (Georgoulis and LaBonte 2007) which, when applied to the SOT magnetogram, gave $\alpha = -0.049 \text{ Mm}^{-1}$.

G) From the theoretical point of view, it will be interesting to examine if some of the loops examined can be modeled by using exact MHD solutions with flows along these loops (Gontikakis et al 2005).

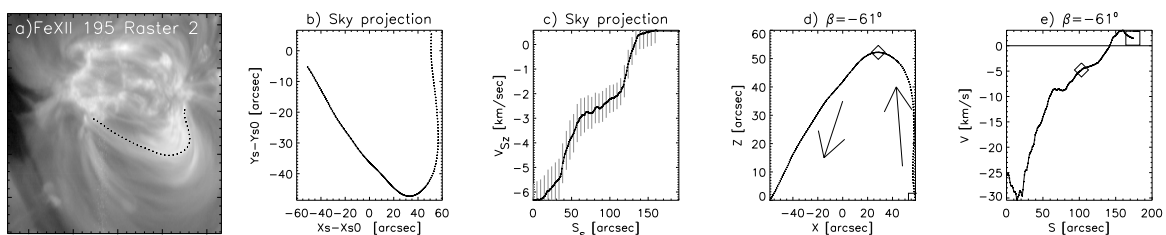


Figure 1: a) Intensity plot of the active region at Fe XII 195Å at raster 2, with the main loop overlaid. b,c) Loop position on the sky plane and line-of-sight velocity as a function of the loop's length. d,e) The reconstructed loop on its own plane (x, z), and the velocity V of the flow along the loop. The diamond symbols show the top of the reconstructed loop, and the box its western footpoint.

References

- [1] Alissandrakis, C.E., 1981: A&A 100, 197-200
- [2] Alissandrakis, C.E, Gontikakis C., Dara, H.C., 2008: Sol. Phys. 252, 73-87
- [3] Del Zanna, G., 2008: A&A 481, L49-L52
- [4] Georgoulis, M.K. and LaBonte, B.J., 2007: Astroph. Journ. 671, 1034-1050
- [5] Gontikakis, C., Petrie, G.J.D., Dara, H.C., Tsinganos, K., 2005: A&A, 434, 1155-1163